Spectrum of Engineering Sciences
ISSN (e) 3007-3138 (p) 3007-312X
Volume 3, Issue 8, 2025

HIGH GAIN METASURFACE ANTENNA FOR 5G WIRELESS COMMUNICATION

Hassan Ibrahim[1], Muhammad Adil[2], Asad Khan[3], Shahid Bashir[4], Bilal Ur Rehman[*5], Kifayat Ullah[6], Muhammad Amir[7], Muhammad Farooq[8]

[1,2,3,4,*5,6,7,8]*Department of Electrical Engineering, University of Engineering and Technology, Peshawar, KPK, Pakistan*

DOI: https://doi.org/10.5281/zenodo.17017459

Keywords
Metasurface, 5G Communication, High Gain, Antenna.

Article History
Received: 28 May, 2025
Accepted: 15 August, 2025
Published: 30 August, 2025

Corresponding Author: *
Bilal Ur Rehman

Abstract
This paper presents the design, simulation, and performance enhancement of a metasurface-based wideband planar antenna tailored for millimetre-wave (mmWave) applications. Based on a metasurface reflector-backed configuration, systematic improvements in antenna performance are achieved by scaling the metasurface array and optimizing the radiating structure. The Simulation results reveal a significant gain enhancement with each design stage: the 3×2 array achieved a gain of 9.46 dBi, the 3×3 modified array yielded 11.22 dBi, and the 4×4 final configuration reached a peak gain of 11.81 dBi. Further, the proposed antenna system offers 17 GHz of impedance bandwidth as compared to the original design, which achieved approximately 15.8 GHz. Also, it highlights the effectiveness of metasurface array optimization as a pathway for gain-focused antenna design without severely compromising impedance bandwidth performance.

INTRODUCTION

With the proliferation of high-speed wireless communication systems, particularly the development and deployment of fifth-generation (5G) networks, there is a significant push toward utilizing higher frequency bands to accommodate the demand for massive data throughput, ultra-low latency, and improved network reliability. Among these frequency bands, the millimetre-wave (mmWave) spectrum, typically ranging from 24 GHz to 100 GHz, has garnered significant attention. The mmWave bands offer the potential for very high data rates and dense spectral reuse. However, the shift to mmWave frequencies also introduces substantial challenges in the design of wireless front-end components, particularly antennas.

Antennas operating at mmWave frequencies must exhibit high gain and directional radiation characteristics due to the increased path losses that naturally occur at higher frequencies. Additionally, compactness and integration capabilities are highly desirable for enabling embedded solutions in base stations, handheld devices, and Internet of Things (IoT) units [1]. The conventional microstrip patch antenna, known for its low profile and ease of integration, suffers from low radiation efficiency and limited gain when scaled to mm-wave frequencies [2]. This limitation necessitates the development of enhanced antenna architectures capable of overcoming the performance bottlenecks inherent in traditional designs.

In this context, metasurfaces have emerged as a transformative solution in modern antenna engineering. Metasurfaces are artificially structured, planar materials composed of subwavelength scatterers arranged in a periodic or quasi-periodic manner. These surfaces can manipulate electromagnetic waves in ways that are unachievable using conventional dielectric or metallic surfaces. When integrated with radiating elements, metasurfaces can enhance gain, directivity, bandwidth, and even polarization characteristics without significantly increasing the antenna's footprint [3]. This property makes them particularly attractive for the design of mmWave antennas for 5G and other high-frequency applications.

The combination of compact radiating elements, such as meander-line structures, with intelligently designed metasurface reflectors presents an innovative pathway toward achieving high-gain, wideband antennas suitable for mmWave communication systems [4]. By exploiting the phase manipulation and impedance tuning

capabilities of metasurfaces, it is possible to improve antenna performance while maintaining design simplicity and fabrication feasibility. This research leverages such an approach to develop a metasurface-based planar antenna capable of addressing the critical requirements of mmWave communication systems.

LITERATURE REVIEW

Traditionally, antenna performance parameters such as gain, bandwidth, and radiation efficiency have been modified by changing the physical structure or geometry of the antenna. These methods include altering the patch shape, substrate material, feeding techniques, and implementing parasitic elements. However, such structural modifications are often limited in their ability to significantly enhance performance without increasing the antenna's footprint or complexity.

This section focuses on the application of metasurfaces to enhance the gain of microstrip patch antennas, particularly in modern communication systems where high gain and compactness are essential. We begin with a detailed review of recent innovations and research efforts in this area, categorized by operational frequency and metasurface integration strategy, followed by a discussion of our own proposed design modifications aimed at gain enhancement.

A new paradigm has evolved because of developments in electromagnetic material science and the appearance of artificially altered materials, referred to as metamaterials and metasurfaces. Because of their special qualities, metamaterials have long drawn the attention of researchers. They can be readily incorporated into a variety of technologies to enhance their intended functionality. Structures with special electromagnetic properties that are not present in nature are known as metamaterial structures. The ability to improve gain, bandwidth, and polarization without requiring large designs or intricate multilayer architectures is one of the new opportunities that these metasurfaces have created in antenna engineering.

On a dielectric layer, a metallic unit cell is usually arranged periodically to create the formations. Metamaterials can be designed in an aperiodic form [5] or with several layers of the same or distinct materials [6]. Using the double negative permeability and permittivity concept, the left-handed metamaterial was created as an example of a metamaterial [7]. Although left-handed metamaterials are not found in nature, they can be created intentionally. Nonetheless, in a particular frequency range, a simultaneous negative value of and can be obtained [8]. Most researchers have designed their studies with the metamaterial's basic properties in mind. An electromagnetic absorber made of metamaterial can be built by taking into account the imaginary part, which also contributes to the loss. The creation of metamaterials as absorbers holds promise for producing electromagnetic devices that function exceptionally well throughout a broad frequency range. Applications of the metamaterial include sub-wavelength imaging, spectroscopy, thermal emission, bolometers, and invisibility cloaks [9]–[13].

To attain high gain for the 28 GHz millimetre wave frequency band, the suggested design in [14] makes use of a metasurface-based methodology. Achieving high gain and CP at millimetre wave frequencies while preserving compact dimensions is a challenge that makes the proposed device unique. A square patch antenna must truncate its corners to achieve circular polarization, which results in two degenerate modes. 6 dBi of gain can be obtained with a single-patch antenna. A metasurface layer based on unit cells is installed in a circular configuration to improve signal reception over the CP antenna.

In contrast to other patch designs like square, triangular, and rectangular, a circular unit cell has the advantage of reducing the effect of losses, such as edge diffraction and scattering, at millimetre-wave frequencies. At 28.6 GHz, the suggested metasurface has increased radiation efficiency to above 80%, giving the antenna a total gain of 11.5 dBi. Because of its small size and characteristics like CP and high gain, the suggested design is ideal for millimetre-wave wireless applications.

Millimetre-wave (mmWave) applications are intended for a wideband planar antenna with a metasurface reflector [15]. The design of the radiation elements uses a straightforward meandering structure, while the parasitic elements and partial ground plane make up the rear side. Due to the use of meander-shaped elements, the antenna's dimensions were tiny. The parasitic elements are used to enhance the impedance matching toward higher frequency bands, while the partial ground plane is utilized to attain a broad bandwidth. Behind the radiating element is a collection of metasurfaces that provide directional radiation characteristics and high gain. Based on the findings of the simulation, the suggested antenna design provides an impedance bandwidth of 17.72GHz within the 22.28–40GHz operational range. The impedance bandwidth, on the other hand, is measured to be 15.8GHz, with a range of 23 to 38.8GHz. Moreover, certain traits are found to be prevalent in a planar antenna based on a metasurface. This study employs this methodology to create a metasurface-based planar

antenna that meets the essential demands of mmWave communication systems.

METHODOLOGY

This research primarily examines the gain of microstrip patch antennas based on the metasurfaces, design of microstrip patch antennas, and unit cell. Figure 1 presents a flow diagram that delineates the systematic methodology employed during the design phase, highlighting the progression from basic design to final implementation.

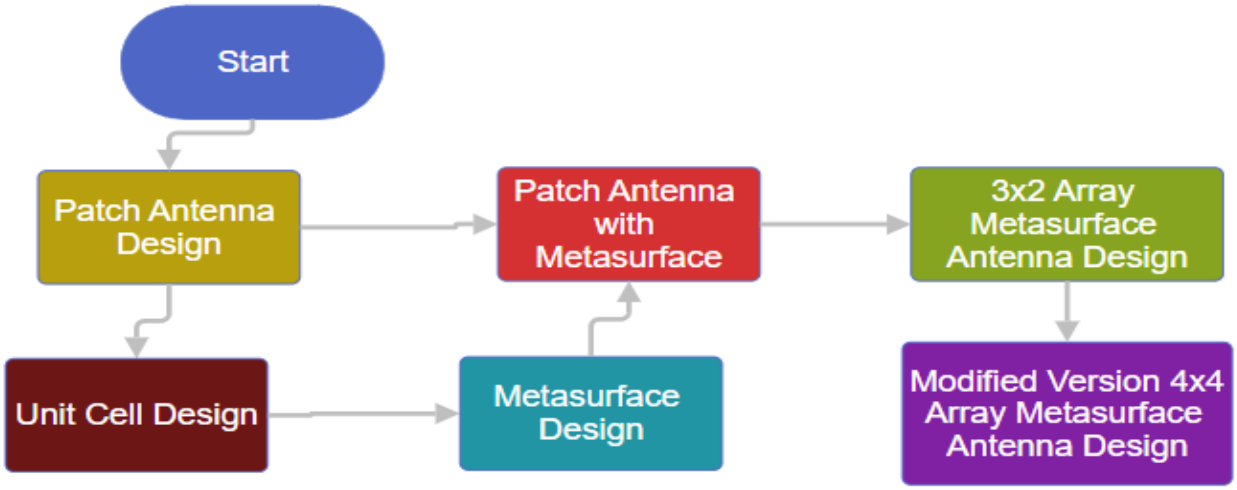

Figure 1: Flow diagram of Methodology

HIGH GAIN METASURFACE INTEGRATED MILLIMETER-WAVE PLANAR ANTENNA

Figures 2(a) and (b) provide illustrations of the suggested wideband planar antenna [16]. A flexible and low-loss Rogers RT/Duroid 5880 substrate serves as the basis for the antenna's design. The antenna design's substrate has a thickness of 0.254 mm. The length of one meandering section is equivalent to one directed wavelength at 26 GHz. A partial ground plane on the antenna's back side is used to provide a broad impedance bandwidth. A 3 × 3 array of parasitic elements, whose primary function is to improve impedance matching in the working bandwidth, is also shown to be positioned just below the radiating element. Additionally, a metasurface reflector is intended enhance. the radiation properties .

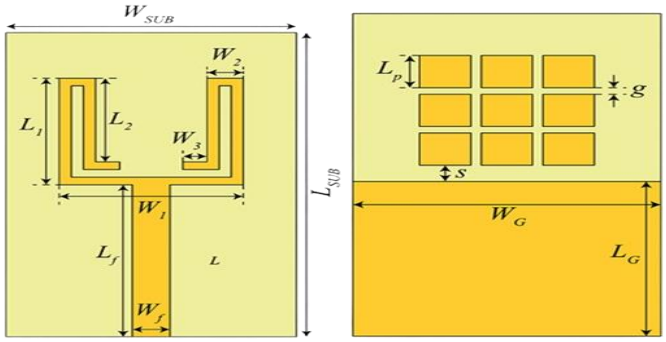

(a) (b)

Figure Error! No text of specified style in document.**: Design of the proposed planar wideband antenna (a) Front view and (b) Rear view [16].**

METASURFACE DESIGN

Figure 3 illustrates the proposed metasurface reflector. It is based on a low-loss Rogers RT/Duroid 5880 dielectric substrate with a thickness of 1.57 mm. A square split ring resonator (SRR) and a circular SRR are utilized, whereas Figure 2(b) features a complete ground plane. The remaining design parameters are: WM = 4, Lp1 = 3.5, Rin = 0.55, d1 = 0.6, d2 = 0.2, g1 = 0.8, and g2 = 0.4 (all measurements in millimeters).

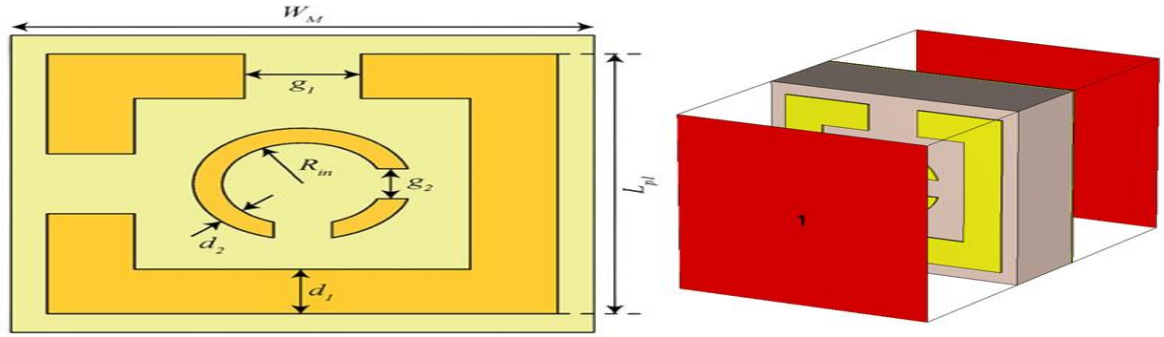

(a) (b)

Figure Error! No text of specified style in document.**: Antenna design (a) Front view and (b) Top view [16]**

In an SRR, the electrical field that is generated is aligned with the no-split bearing side, inducing electric current exclusively on that side. On the contrary, when the electric field is applied along a split bearing side, it causes an electric current in the same side as well as the perpendicular (no split) side. Using this technique, two gaps are introduced in the adjacent sides of the square SRR, one for each linearly polarized impinging field. The inner circular SRR is used to generate plasmon resonances at higher frequencies, thereby achieving a wider bandwidth.

PLANAR ANTENNA WITH METASURFACE

The proposed antenna design, "Meandered Planar Antenna," is developed to attain elevated gain and precise directional radiation features. The configuration of the proposed metasurface integrated planar antenna is illustrated in Figure 4, with a thickness of t=2.5mm. When positioned at a precise distance above the metasurface reflector, the metasurface effectively redirects the antenna's backward radiation to the opposite side. Additionally, the metasurface is positioned underneath the designed antenna to ensure that the back radiation of the antenna is in phase, thus improving the gain. Additionally, a crucial element is the spacing between the antenna and the metasurface reflector, which facilitates the constructive interference of both directly radiated and reflected waves.

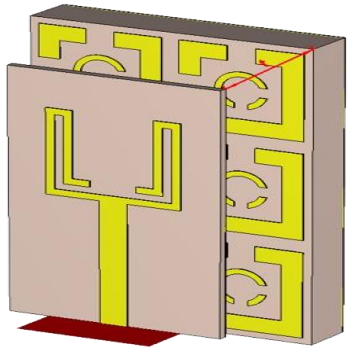

Figure 1: Design of proposed 3×2 array size antenna for t = 2.5mm

In Figures 5 and 6, modify the array size from 3×2 to 3×3, and set the distance between the antenna and the metasurface reflector to t=2.3mm. Further optimization of the metasurface geometry has resulted in an impressive 11.2 dBi, a development that can be linked to enhanced constructive interference and minimized back lobe radiation

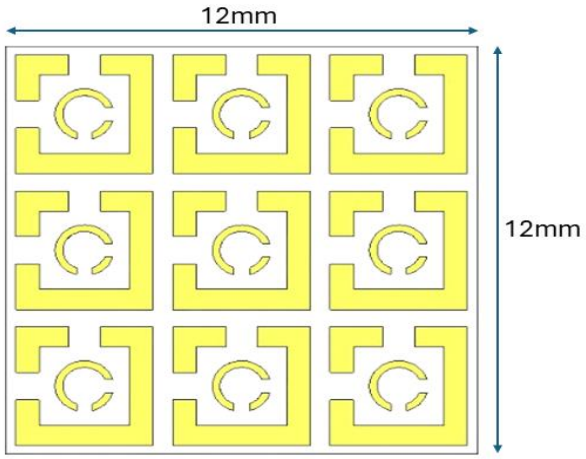

Figure 2: Design of proposed 3×3 array size antenna.

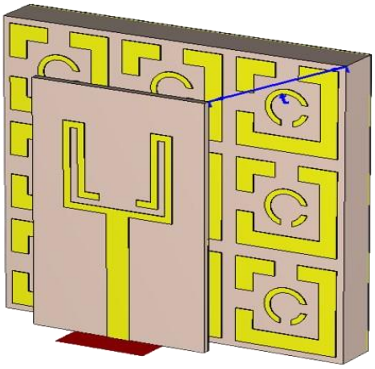

Figure 3: Design of proposed 3×3 array size antenna for t=2.3

Further increasing the array to 4×4 and adjusting the distance between the antenna and metasurface reflector (t=2.5mm), resulting in an enhancement of the gain to 11.8dBi. Figure 7 and Figure 8.

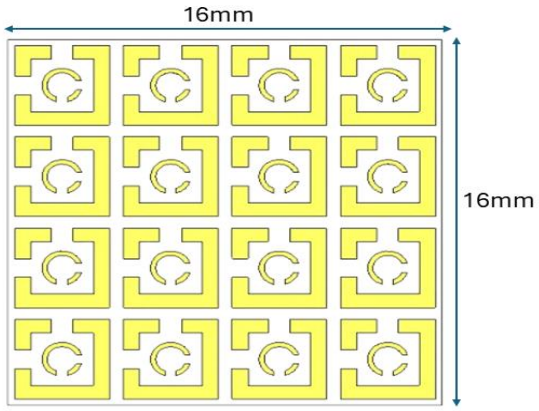

Figure 4: Design of proposed 4×4 array size antenna.

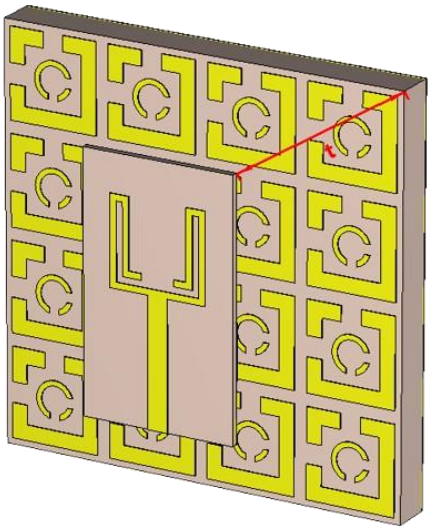

Figure Error! No text of specified style in document.**5: Desing of proposed 4×4 array size antenna for t = 2.5mm**

RESULTS AND DISCUSSION

In this section, the simulation results for the configurations 3×2, 3×3, and 4×4 of the metasurface microstrip patch antenna are presented. Two key parameters, gain and S11 (return loss), serve as crucial indicators of antenna efficiency and suitability. The gain of an antenna reflects its ability to direct radiated energy. The S11 parameter provides insight into how efficiently power is transferred from the transmission line into the antenna. The antennas were evaluated based on their gain and S11 performance, with a particular emphasis on maximizing gain as the primary objective, while recognizing that a moderate trade-off in S11 is acceptable for practical implementation.

A. Unit Cell Analysis

a) **S11 Parameter**

In a square split ring resonator, the applied electric field is parallel to the non-split bearing side and generates electric current on the same side only. On the contrary, when the electric field is applied along a split bearing side, it causes an electric current on the same side as well as the perpendicular (no split) side. Using this technique, two gaps are introduced in the adjacent sides of the square split ring resonator, one for each linearly polarized impinging field. The inner circular SRR is used to generate plasmon resonances at higher frequencies, thereby achieving a wider bandwidth. The simulated S-parameters of the proposed metasurface are depicted in Figure 9. The metasurface operates well from 20 to 35GHz, according to the -3 dB bandwidth criteria, which covers the operating band of interest.

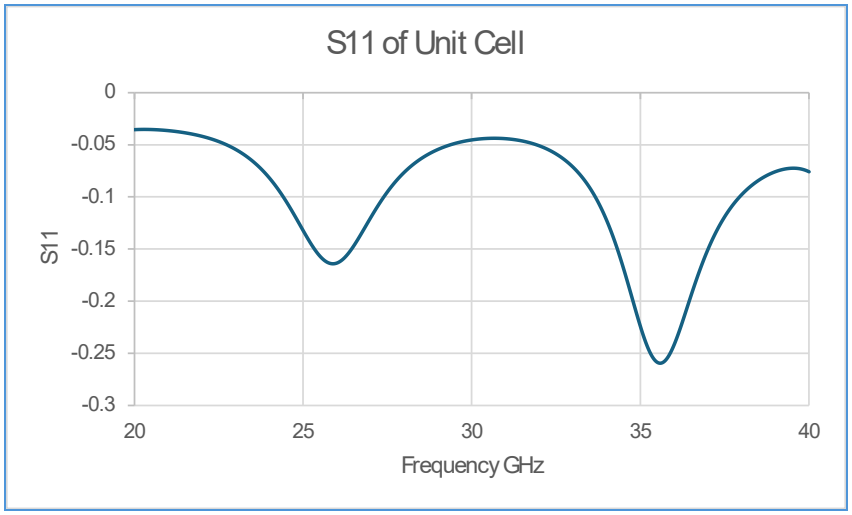

Figure Error! No text of specified style in document.**9: S11 parameter for Unit Cell**

2) **Efficiency of the Unit Cell**

The total efficiency graph of the unit cell in Figure 10, plotted across a frequency range of 20 GHz to 40 GHz, exhibits moderate variation, indicating stable performance within this band. The efficiency expressed in decibels (dB) remains close to 0 dB throughout the range, with a minimum around 35 GHz, reaching approximately -0.27 dB. This dip suggests a slight reduction in radiated efficiency at that frequency. Conversely, a local peak near 30 GHz, around -0.05 dB, signifies a region of enhanced performance. Overall, the graph demonstrates that the unit cell maintains high efficiency (above -0.25 dB) across the band, making it suitable for high-frequency applications, particularly in the 5G mmWave range. These minor efficiency variations imply minimal power loss, which is critical for maintaining the integrity of the transmitted signal and achieving the high-gain objectives of the metasurface antenna design.

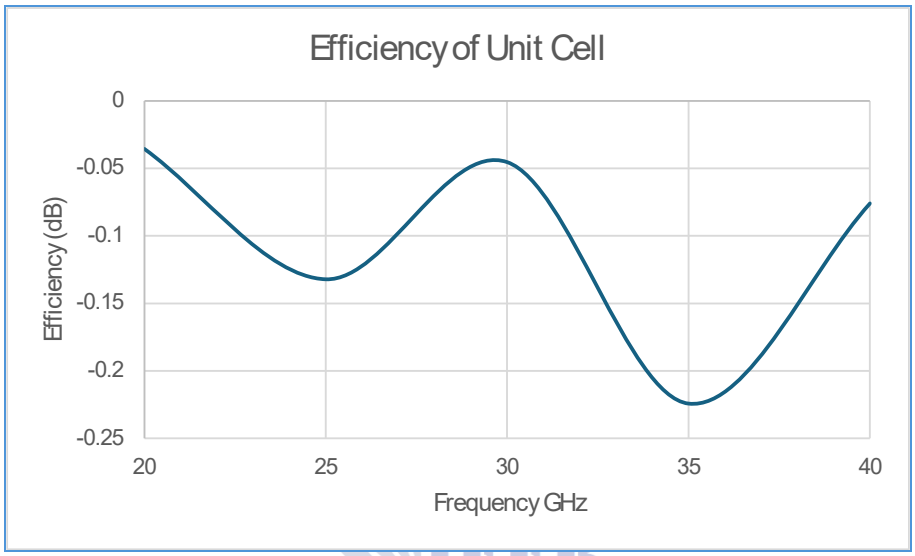

Figure Error! No text of specified style in document.**10: Efficiency of the proposed Unit Cell**

3) **Far Field Radiation Patterns of Unit Cell**

The far-field radiation patterns of the unit cell as shown in Figure 11, evaluated at 25 GHz, 30 GHz, and 35 GHz, demonstrate consistent directional behaviour and effective radiation characteristics across the frequency range. At all three frequencies, the main lobe is directed along 0 degrees, indicating a stable broadside radiation pattern, which is ideal for metasurface-based antenna arrays. The main lobe magnitude increases progressively with frequency, from 16.1 dB(V/m) at 25 GHz to 18.9 dB(V/m) at 35 GHz, reflecting an enhancement in radiated field strength. Additionally, the angular width (3 dB) remains relatively constant, ranging from 129.3° to 131.9°, implying consistent beamwidth performance and efficient spatial coverage. These results affirm that the unit cell maintains robust radiation properties over the operational frequency band, supporting its suitability for integration into high-gain 5G mmWave antenna designs

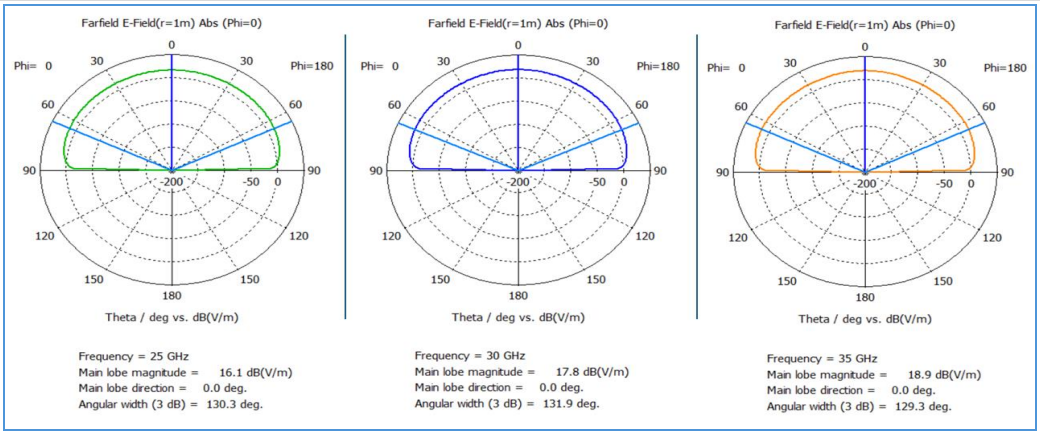

Figure Error! No text of specified style in document.**: The far-field radiation patterns for 25 GHz, 30 GHz, and 35 GHz (phi=0)**

The far-field radiation patterns at Phi = 90° for 25 GHz, 30 GHz, and 35 GHz as shown in Figure 12, validate the directional and stable performance of the unit cell across the targeted frequency range. At all three frequencies, the main lobe direction remains fixed at 0°, confirming consistent broadside radiation in the H-plane. The main lobe magnitude improves with increasing frequency, from 16.1 dB(V/m) at 25 GHz to 18.9 dB(V/m) at 35 GHz, aligning with the desired high-gain characteristics. The 3 dB angular width slightly broadens from 80.4° to 85.4°, maintaining a focused beam while supporting moderate angular coverage. Significantly, the side lobe levels decrease with frequency, from -1.7 dB at 25 GHz to -3.4 dB at 35 GHz, indicating enhanced radiation efficiency and reduced power leakage in undesired directions. This suppression of side lobes is critical for minimizing interference and improving overall antenna performance, making the unit cell well-suited for integration in high-frequency metasurface antennas used in 5G applications.

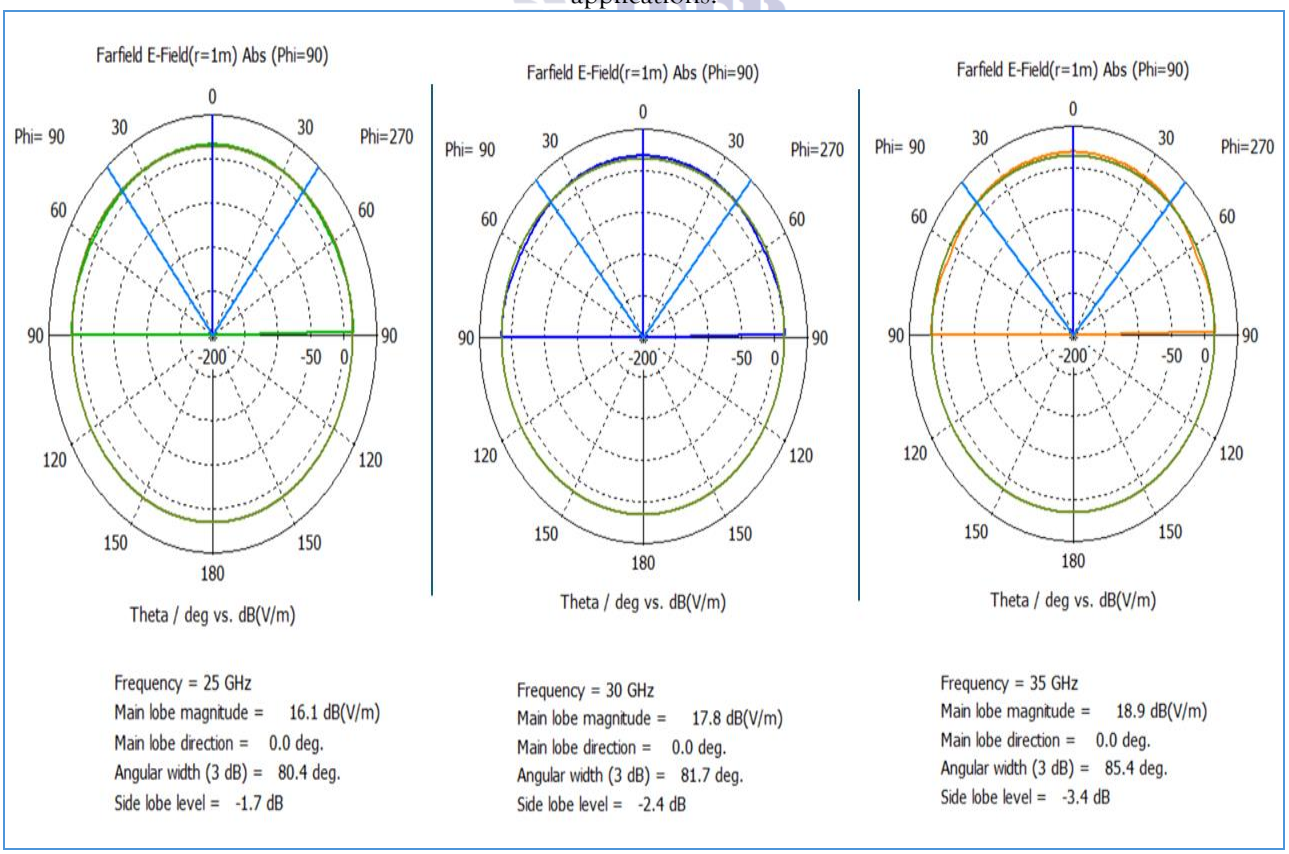

Figure Error! No text of specified style in document.**: The far-field radiation patterns for 25 GHz, 30 GHz, and 35 GHz (phi=90)**

4) **Results of 3x2, 3x3, 3x4 Array Patch Antennas**

The results summarized in Table 1 show a clear improvement in the antenna performance with increasing array size and design modifications. Specifically, the gain of the antenna improves as the array size increases from 3×2 to 4×4. The 3×2 array antenna with metasurface achieves a gain of 9.46 dBi, while the 3×3 modified version reaches 11.22 dBi. The final 4×4 modified antenna with metasurface achieves the highest gain of 11.81 dBi. This upward trend in gain demonstrates the effectiveness of using larger arrays and metasurface modifications to enhance antenna performance in terms of directional signal strength, which is essential for applications like 5G communication, where high gain is critical for reliable data transmission.

TableError! No text of specified style in document. **1: Comparison of Gain Results in different array antennas**

Antenna Configuration	Gain (dBi)
3x2 Array Antenna with Metasurface	9.46
3×3 Array Modified Antenna with Metasurface	11.22
4×4 Array Modified Antenna with Metasurface (Final version)	11.81

In terms of S11 (reflection coefficient) and bandwidth performance, the results indicate that increasing the array size and optimising the antenna structure led to better impedance matching and slightly reduced bandwidth. The minimum S11 value becomes more negative from -18.74 dB in the 3×2 array to -28.43 dB in the 4×4 array, reflecting a significant reduction in signal reflection and better energy transmission. However, this improvement comes with a slight reduction in bandwidth, decreasing from approximately 18 GHz in the 3×2 array to around 16 GHz in the 4×4 array. This trade-off is acceptable in many high-frequency applications where achieving high gain and good impedance matching is more critical than maintaining a wide bandwidth. Also, the comparison of S11 and bandwidth is provided in Table 2.

Table 2: Comparison of S11 and Bandwidth of 3x2, 3x3, 3x4 Array Patch Antennas

Antenna Configuration	Minimum S11 (dB)	Resonant Frequency (GHz)	Bandwidth (–10 dB)
3×2 Array Antenna with Metasurface	–18.74	27.2	~18GHz
3×3 Array Modified Antenna with Metasurface	–22.68	26.6	~17 GHz
4×4 Array Modified Antenna with Metasurface (Final version)	–28.43	26.8	~16 GHz

5) **Discussion**

Gain Analysis

Gain is a direct measure of how well an antenna radiates energy in a desired direction. It is particularly crucial for applications requiring long-range communication, strong signal strength, or high throughput, and the core demands of 5G networks. Without a metasurface, the Antenna gives a gain of 4.5 dBi as shown in Figure 13.

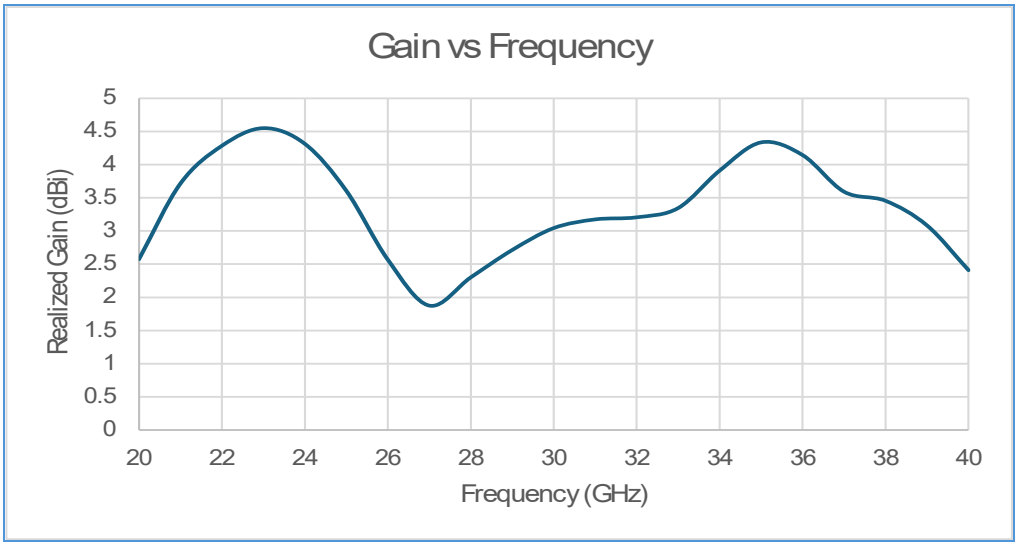

Figure 13: Gain for Antenna without Metasurface

The 3×2 array exhibited a gain of 9.46 dBi, as in Figure 14, serving as a baseline design. While suitable for short-range or compact applications, its limited aperture area constrained its beamforming capability and radiation efficiency.

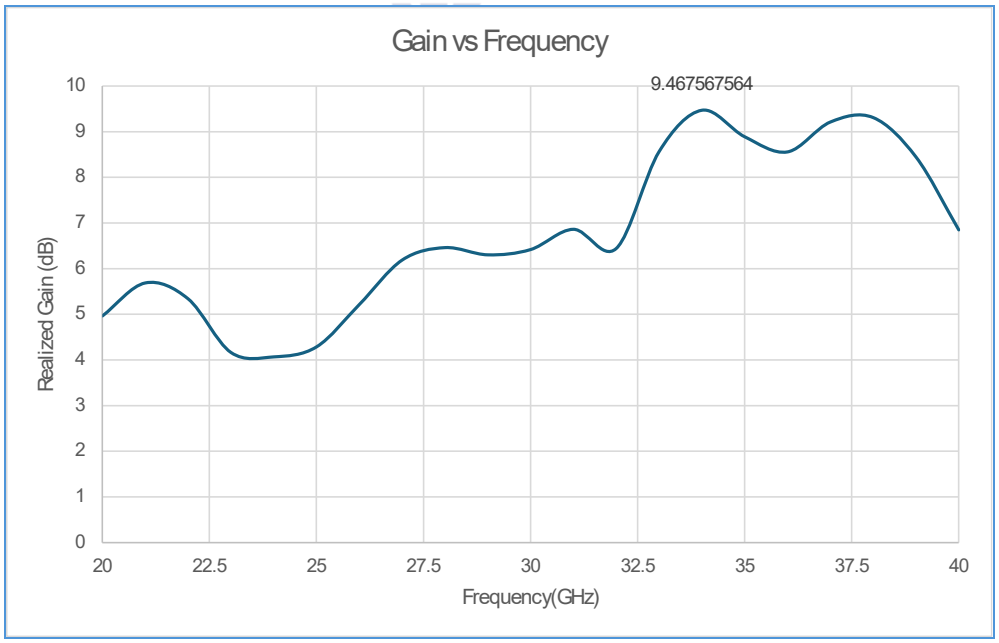

Figure 14: Gain vs Frequency for 3×2Array.

The 3×3 modified array demonstrated a considerable gain improvement to 11.22 dBi, as in Figure 15, signifying the success of metasurface and structural modifications. This enhancement (˜1.76 dBi over the 3×2 design) is attributed to better electromagnetic wave management through optimised unit cell arrangement and inter-element spacing. The result shows how a relatively small increase in array size, combined with design tweaks, can lead to significant radiation improvements.

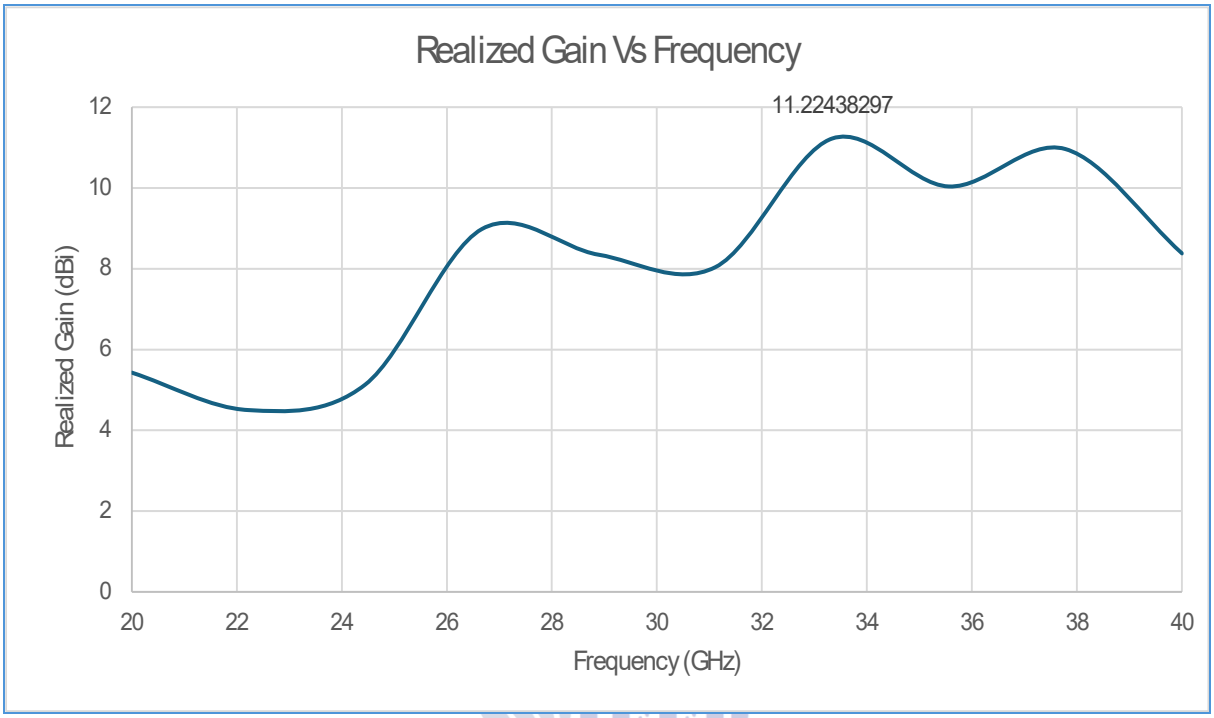

Figure 15: Gain vs Frequency for 3×3 Array.

The proposed 4×4 array design provides the highest gain of 11.81 dBi, as in Figure 16, confirming the effectiveness of scaling up the antenna array. While the incremental gain over the 3×3 version is smaller (˜0.59 dBi), it represents a refinement toward optimal beam shaping and radiative efficiency. The 4×4 structure, due to its larger aperture and increased element count, focuses the energy more tightly and minimises side lobe levels. By applying a parametric sweep on the distance (t) between the patch antenna and the Metasurface, we get two results. For t=2.5, we get 11.44 dBi, and for t=2, we get 11.81 dBi, which is good.

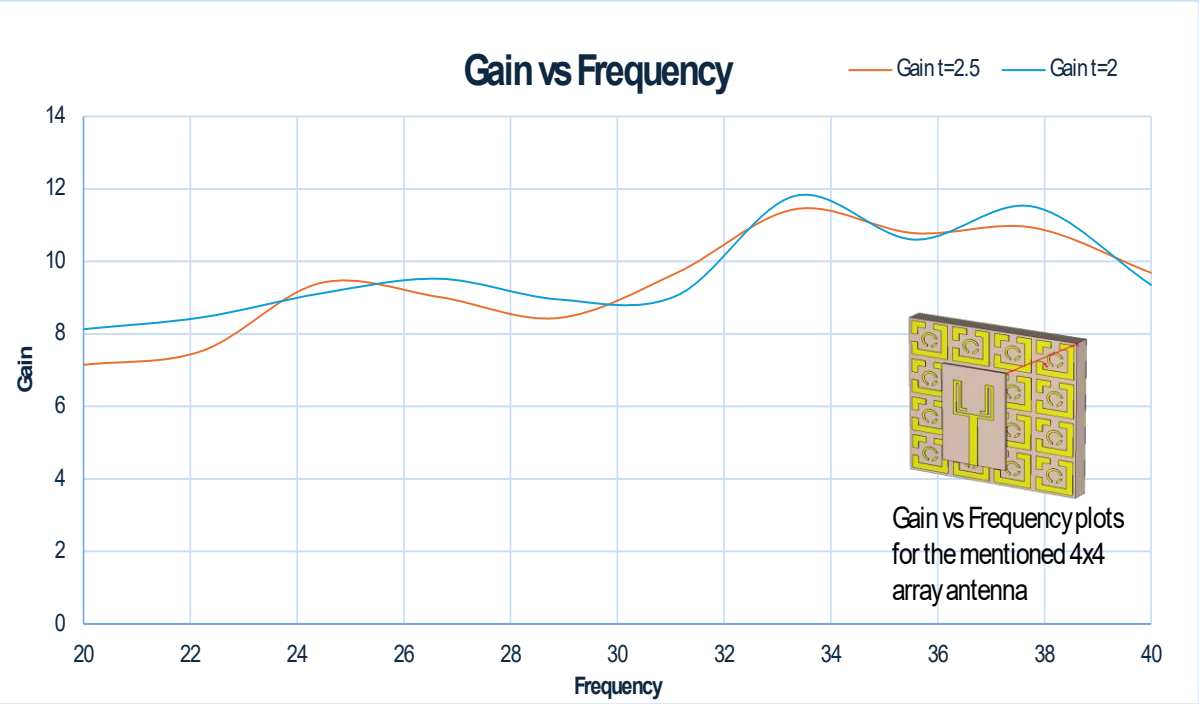

Figure 16: Gain vs Frequency for 4×4 Array

From the above configurations, gain increases with array size and design of the antenna architecture.

S11 (Return Loss) Analysis

The S11 parameter indicates how much input power is reflected due to impedance mismatch. For efficient radiation, S11 should ideally be below –10 dB at the operating frequency, ensuring at least 90% of the input power is radiated. Without a metasurface, the Antenna gives S11 as shown in Figure 17.

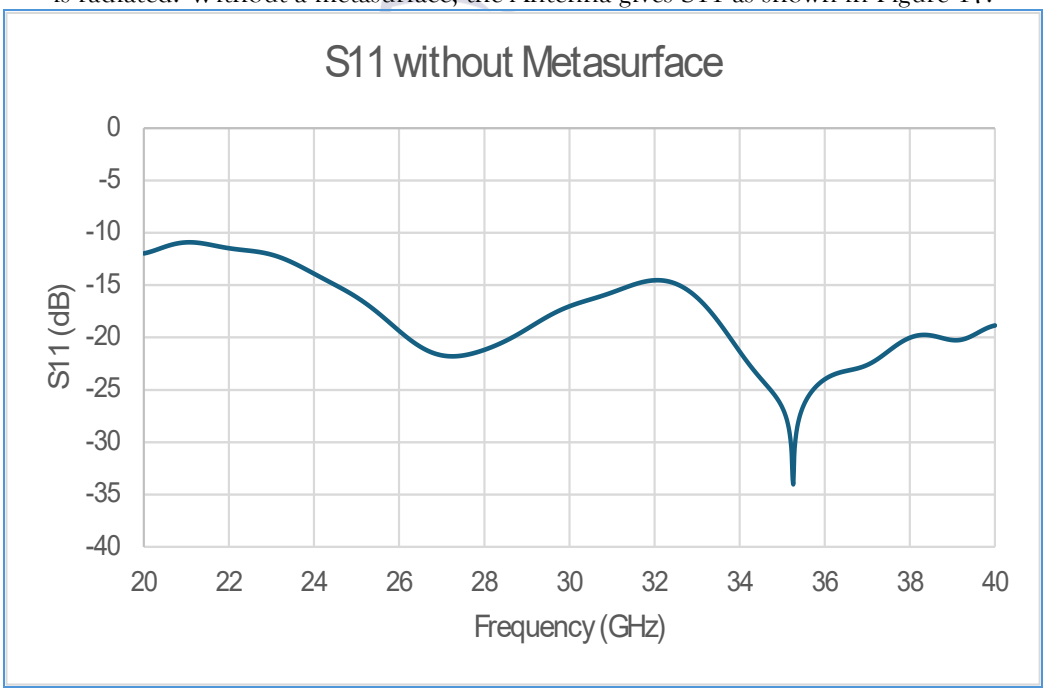

Figure 17: S11 for Antenna without Metasurface

The 3×2 antenna achieved a minimum S11 of -18.74 dB at 27.2 GHz, as shown in Figure 18, indicating a decent impedance match and efficient energy transfer at the resonant frequency. The bandwidth of ~2.4 GHz, although narrow, is acceptable for focused-band applications.

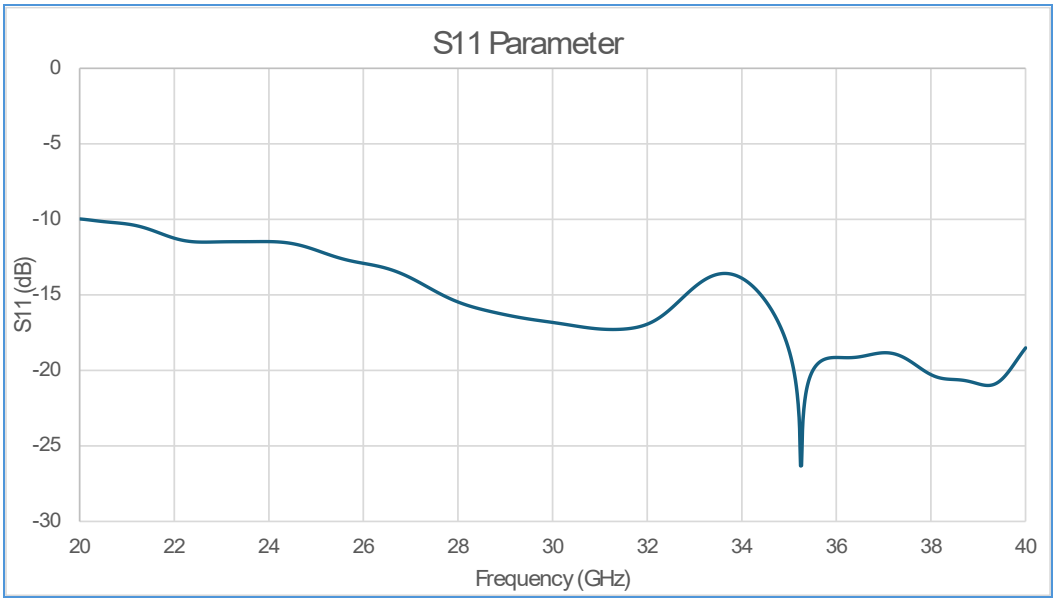

Figure 18: S11 for 3×2 Array.

The 3×3 modified design improved the S11 to –22.68 dB as in Figure 19, along with a broader bandwidth of ~3.2 GHz, centred around 26.6 GHz. Hence, it suggests not only a better impedance match but also increased operational flexibility. The improvement in S11 corresponds well with the gain boost, indicating that design properties.

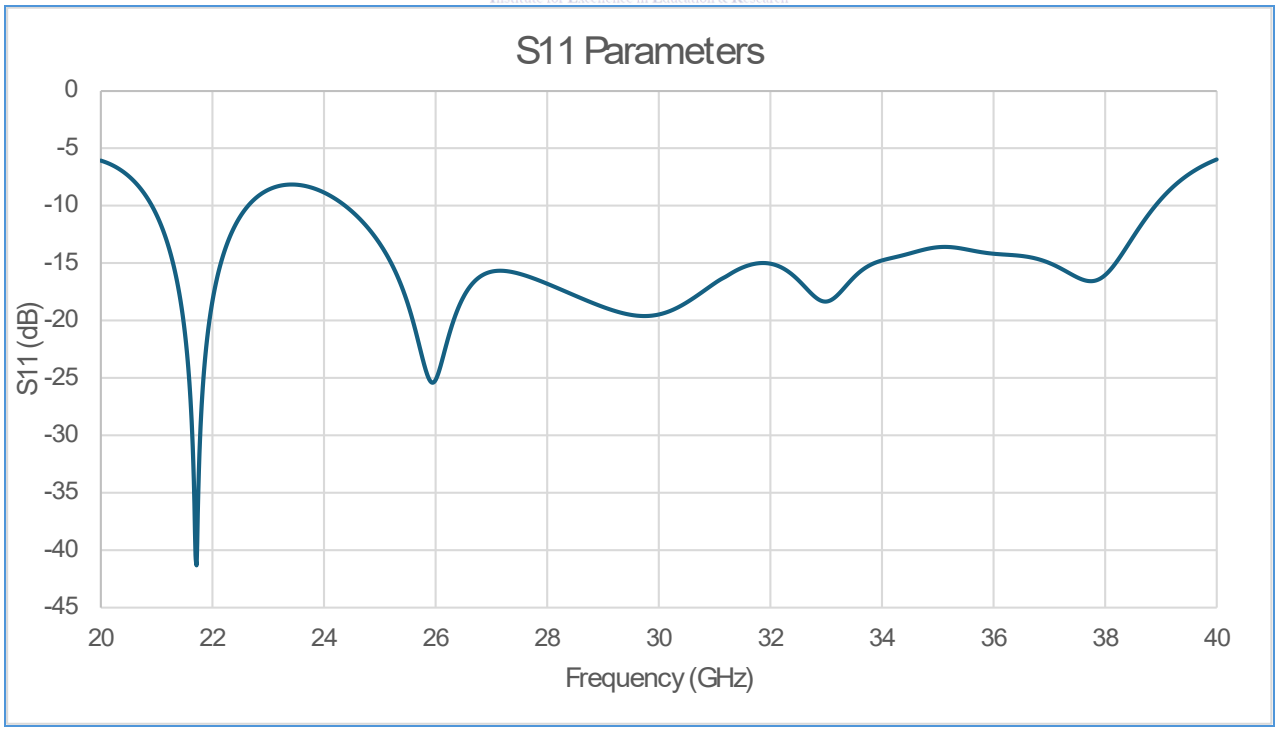

Figure 19: S11 for 3×3 Array.

The 4×4 final version reached an excellent S11 of -28.43 dB at 26.8 GHz, as shown in Figure 20, with the broadest bandwidth of ~4.5 GHz. Hence, it means that all the input power is utilized for radiation, with minimal losses due to reflection. Such wideband performance makes this antenna suitable for broadband and multi-frequency systems.

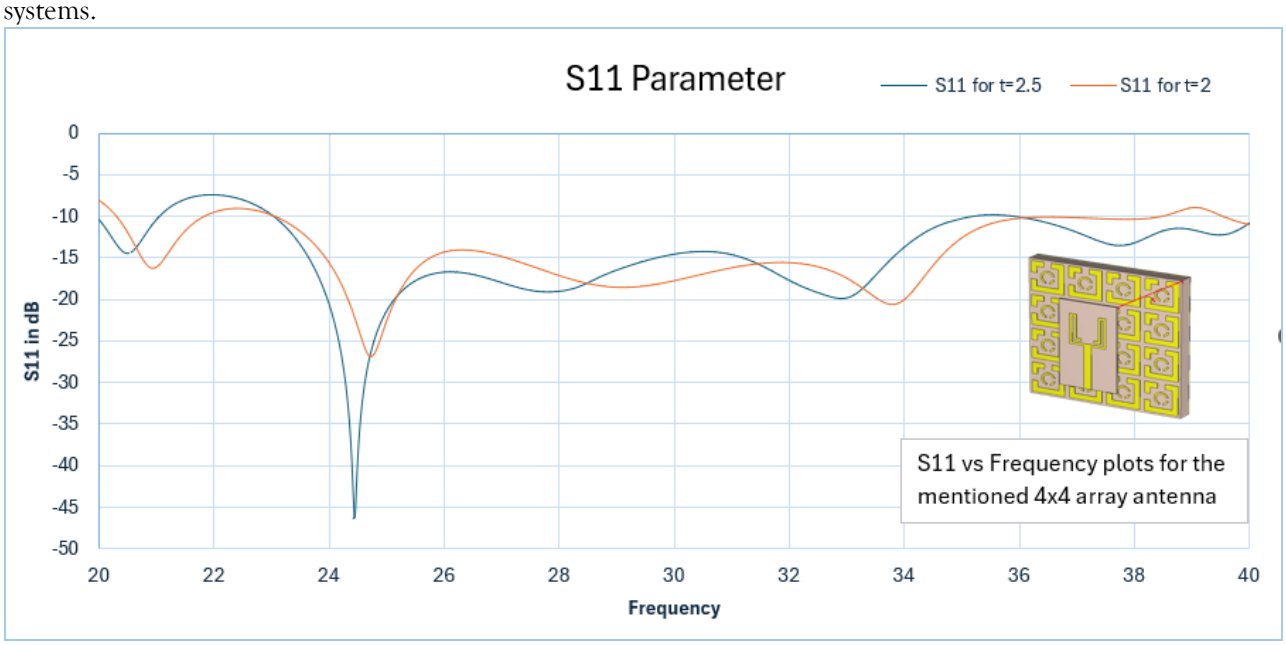

Figure Error! No text of specified style in document. **S11 for 4×4 Array (Final version)**

However, it is important to note that S11 performance, while important, is not the primary objective in this study. Our main focus is on achieving higher gain, even if it necessitates minor compromises in return loss.

Comparative Anaylsis

The comparative analysis of the three metasurface antenna designs demonstrates a clear, consistent trend: larger and optimized arrays produce higher gain, while also supporting better or comparable S11 performance.

- The 3×2 array is a simple, baseline design with moderate gain and satisfactory return loss.
- The 3×3 modified array introduces structural improvements that elevate both gain and bandwidth.
- The 4×4 final version is the most efficient design, achieving the highest gain and excellent S11, making it ideal for high-performance wireless systems.

From a thesis standpoint, the study achieves its primary objective: to enhance antenna gain using metasurface-based design strategies while maintaining practical S11 levels.

CONCLUSIONS

In this research, a metasurface-enabled microstrip patch antenna is employed to enhance the gain in the mmWave spectrum, specifically at 26 GHz. The baseline microstrip patch antenna showed a simulated gain of 4.5 dBi, whereas the metasurface-enhanced design yielded a peak gain of 10.8 dBi, marking a gain enhancement of approximately 4.6 dB. Additionally, the –10 dB impedance bandwidth remained within acceptable limits for 5G applications, spanning from 25.6 GHz to 26.4 GHz. These results validate the effectiveness of metasurfaces in directing and reinforcing radiation in desired directions without significantly compromising bandwidth or return loss, which remained around -22 dB at resonance. In future work, the development of reconfigurable metasurfaces using tunable components like varactor diodes or MEMS switches can further increase the performance in terms of gain.

REFERENCES

[1] Garg, B. and D. Saleem, Experimental verification of double negative property of LHM with significant improvement in microstrip transceiver parameters in S band International Journal of Engineering Practical Research (IJEPR), Vol. 2, No. 2, 6470, 2013.

[2] Schurig, D., J. J. Mock, B. J. Justice, S. A. Cummer, J. B. Pendry, A. F. Starr, and D. R. Smith, Metamaterial electromagnetic cloak at microwave frequencies, Science, Vol. 314, 977980, 2006.

[3] Chang, Y. C., C. M. Wang, M. N. Abbas, M. H. Shih, and D. P. Tsai, T-shaped plasmonic array as a narrow band thermal emitter or biosensor, Optics Express, Vol. 17, No. 16, 1352613531, 2009.

[4] Huang, L. and H. Chen, Multi-band and polarization insensitive metamaterial absorber, Progress In Electromagnetics Research, Vol. 113, 103 110, 2011.

[5] Chen, H. S., L. Huang, X. X. Cheng, and H. Wang, Magnetic properties of metamaterial composed of closed rings, Progress In Electromagnetics Research, Vol. 115, 317326, 2011.

[6] Kim, D.-S., D.-H. Kim, S. Hwang, and J.-H. Jang, Broadband terahertz absorber realized by self-assembled multi-layer glass spheres, Optics Express, Vol. 20, No. 12, 1356613572, 2012.

[7] Majid, H. A., M. K. A. Rahim, and T. Masri, Left-handed metamaterial design for microstrip antenna application, 2008 IEEE International RF and Microwave Conference Proceeding, 218 221, 2008.

[8] Shi, Y. and C.-H. Liang, The analysis of double-negative materials using multi-domain pseudo spectral time-domain algorithm, Progress In Electromagnetics Research, Vol. 51, 153165, 2005.

[9] Schurig, D., J. J. Mock, B. J. Justice, S. A. Cummer, J. B. Pendry, A. F. Starr, and D. R. Smith, Metamaterial electromagnetic cloak at microwave frequencies, Science, Vol. 314, 977980, 2006.

[10] Huang, Y., G. wen, and W. Zhu, Experimental demonstration of a magnetically tunable ferrite-based metamaterial absorber, Optics Express, Vol. 22, No. 13, 1640816417, 2014.

[11] Liu, X. L., L. P. Wang, and Z. M. Zhang, Wideband tunable omnidirectional infrared based on doped-silicon nanowire arrays, Journal of Heat Transfer, Vol. 135, No. 6, 061602, 2013.

[12] Chang, Y. C., C. M. Wang, M. N. Abbas, M. H. Shih, and D. P. Tsai, T-shaped plasmonic array as a narrow band thermal emitter or biosensor, Optics Express, Vol. 17, No. 16, 1352613531, 2009.

[13] Zhao, J., Y. Feng, B. Zhu, and T. Jiang, Sub-wavelength image manipulating through compensated anisotropic metamaterial prisms, Optics Express, Vol. 16, No. 22, 18057 18066, 2008.

[14] P. H. Lakshman, Y. Thatti, P. K. T. Rajanna, and S. Mudukavvanavar, "High-gain circularly polarized metasurface antenna for NR257 band millimeter-wave 5G"

[15] M. J. Jeong, N. Hussain, J. W. Park, S. G. Park, S. Y. Rhee, and N. Kim, "Millimeter-wave microstrip patch antenna using vertically coupled split ring metaplate for gain enhancement," *Microwave Opt Technol Lett*, vol. 61, no. 10, pp. 2360–2365, Oct. 2019.

[16] M. U. Tahir, U. Rafique, M. M. Ahmed, S. M. Abbas, S. Iqbal, and S.-W. Wong, "High gain metasurface integrated millimeter-wave planar antenna," *Int. J. Microwave Wireless Technol.*, vol. 16, no. 2, pp. 306–317, 2024.